RSC Advances

PAPER

View Article Online
View Journal | View Issue

Cite this: *RSC Adv.*, 2017, **7**, 28940

High yield production of C_2–C_3 olefins and *para*-xylene from methanol using a SiO_2-coated FeO_x/ZSM-5 catalyst†

Qiongfang Hu,[a] Xiaofan Huang,[bc] Yu Cui,[ab] Tengfa Luo,[c] Xiaoping Tang,[ab] Tong Wang,[abc] Weizhong Qian *[a] and Fei Wei [a]

Received 11th April 2017
Accepted 19th May 2017

DOI: 10.1039/c7ra04111j

rsc.li/rsc-advances

Herein, FeO_x-supported ZSM-5 exhibited excellent catalytic performance in the aromatization of methanol, similar to ZnO_x-supported ZSM-5 but with much longer life time. Coating of FeO_x/ZSM-5 catalyst with a SiO_2 shell is effective to suppress the isomerization of xylene and hydrogen transfer from propylene to propane on the external surface. As a result, FeO_x/ZSM-5@SiO_2 exhibited gross yield of C_2–C_3 olefins and *para*-xylene (carbon base) far higher than that of HZSM-5, ZnO_x/ZSM-5, and ZnO_x/ZSM-5@SiO_2.

Transformation of methanol on zeolite remained a hot catalytic field in the last two decades, owing to its importance in providing C_2–C_3 olefins and aromatics, which are key building blocks in the chemical industry.[1–7] Although numerous efforts were made in solely improving the selectivity of olefins or aromatics, there always existed both olefins and aromatics in the product,[1,4–8] owing to the intrinsic dual hydrocarbon pool mechanism of conversion of methanol inside HZSM-5.[9–12] Considering that both C_2–C_3 olefins and aromatics, especially *para*-xylene (PX), belong to the most valuable products in hydrocarbons, it is also a good choice to achieve high gross yield of them. While realizing this goal in a methanol-to-aromatics (MTA) reaction, it is crucial to increase the single pass yield of PX and C_2–C_3 olefins by maintaining high aromatization ability, as well as suppressing various reactions including dealkylation, alkylation, and isomerization of xylene (X) and the hydrogen transfer from olefins to paraffins.[4,13–18] The widely investigated catalysts in the MTA process included ZnO_x-, AgO- or Ga_2O_3-doped ZSM-5.[13–19] Among these, ZnO_x/ZSM-5 has received significant attention since Ag is too expensive and Ga_2O_3 is toxic and has very low reserve in the earth. Definitely, ZnO_x interacted with ZSM-5 to create Lewis acids sites in high density on the catalyst,[1,22,23] resulting in the increase of aromatization ability, compared to that of HZSM-5. However, ZnO_x-doped ZSM-5 (microsized) always suffered from the limitation of rapid deactivation within 1–2 hours.[13] Nanosized ZSM-5 or hierarchical structures of ZSM-5 were used to enhance the diffusion of the intermediate products outside the pores.[15–21] However, the excess alkylation of xylene (X) occurred on the huge external surface of nanocrystals, resulting in very low yield of PX.[15–21] In addition, another disadvantage of ZnO_x for use in fluidized beds is the formation of a spinel of $ZnAl_2O_4$ when it interacts with alumina gel, as reported previously.[13,18,24,25]

In the present study, we proposed FeO_x-doped ZSM-5 as a new platform of MTA. The acidity information was compared with that of ZnO_x/ZSM-5. In addition, both FeO_x/ZSM-5 and ZnO_xZSM-5 were coated with SiO_2 shell to supress the external acids and the associated isomerization of X. The catalytic performances, including the conversion of methanol, yield of aromatics, selectivity of PX in X, yield of PX, and effect on the hydrogen transfer of C_2–C_3 olefins (to paraffins) were discussed based on HZSM-5, ZnO_x-based, and FeO_x-based catalysts. SiO_2-coated FeO_x/ZSM-5 exhibited longer life time to produce C_2–C_3 olefins and PX in the highest gross yield among all the catalysts tested. The shorter life time of ZnO_x-based catalysts is due to high density of Lewis acids as compared to those of HZSM-5 and FeO_x-based catalysts. The present study not only provides the clues for the variation of C_2–C_3 olefins and PX influenced by the external acids but also provides a new catalyst platform for MTA reaction for the control of the product selectivity.

Experimentally, HZSM-5 with a Si/Al ratio of 12.5 and average size of 2 micrometers (purchased from Nankai Catal. Corp., China) was doped with a solution of $Fe(NO_3)_3$ under stirring for 5 hours. Then, the mixture was dried at 110 °C for 12 hours to evaporate water and calcined at 550 °C for 5 hours. The catalyst was denoted as FeO_x/ZSM-5. Loading of FeO_x, calculated by Fe, is 4.2% on ZSM-5.

Similarly, solutions of $Zn(NO_3)_2$ were impregnated on ZSM-5 powders following the same drying and calcination procedures

[a]*Department of Chemical Engineering, Tsinghua University, 100084, China. E-mail: qianwz@tsinghua.edu.cn*

[b]*Coal Chemical Industry Division, Huadian Coal Industry Group Co. Ltd., Beijing 100031, China*

[c]*Shanxi Yuheng Chemical Co., Huadian Coal Industry Group Co. Ltd., Yulin, 719000, Shanxi, China*

† Electronic supplementary information (ESI) available: TEM images of catalysts, TPR pattern of FeO_x/ZSM-5, NH_3-TPD data of catalysts. See DOI: 10.1039/c7ra04111j

to obtain a catalyst denoted as ZnO_x/ZSM-5. Loading of ZnO_x, calculated by Zn, is 3% on ZSM-5, in agreement with the optimized value reported in previous work.[4,21] To create a SiO_2 shell on the external surface, the catalyst powders were soaked in the solution of TEOS in cyclohexane under stirring for 5 hours.[4] Then, the mixture was dried at 110 °C for 24 hours, and the powders were calcined at 550 °C for 5 hours. The catalysts with a SiO_2 shell are denoted as ZnO_x/ZSM-5@SiO_2 and FeO_x/ZSM-5@SiO_2. NH_3-TPD and Py-IR were used to obtain information about the acidity of different catalysts.[4] Probe molecule of 2,6-di-*tert*-butylpyridine was used to quantitatively determine the density of external acids of different catalysts (ESI-1, Fig. S1†). To obtain the yield of C_2–C_3 olefins and PX from methanol, 1 g of the catalyst was placed into a quartz-made packed bed reactor to decompose methanol at 475 °C and ambient pressure. Space velocity of methanol is 0.79 g g_{cat}^{-1} h^{-1}. All gaseous products were online analysed by the GC. The yield of hydrocarbons was calculated with the carbon base.

TEM characterization indicated that ZnO_x species were monodispersed into the matrix of ZSM-5. Only the crystals of ZSM-5 were observed in the TEM image (ESI-2, Fig. S2†). However, for the doping of FeO_x species on ZSM-5, the crystals of Fe_2O_3 can be clearly observed in the TEM image (ESI-1, Fig. S3†). TPR of FeO_x/ZSM-5 suggested that FeO_x is only partly reduced at the reaction temperature of 475 °C in the MTA reaction (ESI-3, Fig. S4†). It validated that it is FeO_x, not metallic Fe, that interacts with ZSM-5. The coating method of ZnO_x-based or FeO_x-based ZSM-5 by SiO_2 is similar to that reported in previous work,[4] giving a SiO_2 shell thickness around 8 nm. NH_3-TPD was used to determine the strength and density of the acid sites of HZSM-5, FeO_x^-, and ZnO_x-supported ZSM-5 (Fig. 1a). The peak at 200–250 °C is the contribution of the hydrogen bond of NH_4^+, assigned to the weak acid sites. Another peak of HZSM-5 at 542.9 °C was assigned to the strong acid sites. This peak (at 542 °C) disappeared after ZnO_x or FeO_x were doped in ZSM-5. However, peak areas between 300 °C and 500 °C increased after the doping, which were associated with the medium strong acids. Quantitatively, peak areas at 227.3, 315.6, and 542.9 °C for HZSM-5 contributed to 25.3%, 60.6%, and 14.1%, respectively (ESI-4, Table S1†). Peak areas at 224.7, 267.8, and 328.9 °C for FeO_x/ZSM-5 contributed to 9.0%, 36.8%, and 54.2%, respectively. In comparison, peak areas at 221.4, 266.2, and 342.7 °C for ZnO_x/ZSM-5 contributed to 11.1%, 6.5%, and 62.4%, respectively. The medium strong acids for ZnO_x/ZSM-5 had a higher density with a peak temperature 14 °C higher than that of FeO_x/ZSM-5. Similarly, the medium strong acids for FeO_x/ZSM-5 had a peak temperature 14 °C higher than that of HZSM-5. Doping of metal oxides not only changed the peak position and acidic strength discussed above, but also significantly decreased the acid density (ESI-5, Table S2†). These differences would exhibit different effects on the catalytic performances discussed below.

Py-IR suggested that peaks of the Brönsted acids of HZSM-5, centred at 1540 cm^{-1}, almost disappeared for ZnO_x/ZSM-5 (Fig. 1b), but most of them were retained after doping of FeO_x. Coating of the catalyst by the SiO_2 shell resulted in the decrease of both the Brönsted acids and Lewis acids, whether

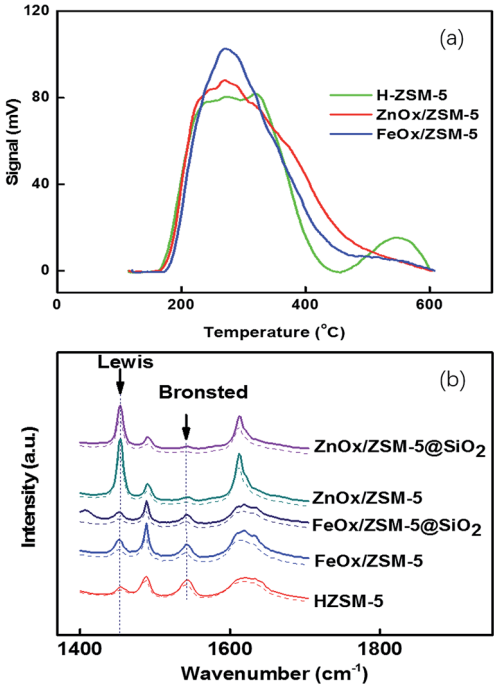

Fig. 1 (a) NH_3-TPD spectrum of HZSM-5, ZnO_x/ZSM-5 and FeO_x/ZSM-5. (b) Py-IR spectrum of HZSM-5, FeO_x/ZSM-5, FeO_x/ZSM-5@SiO_2, ZnO_x/ZSM-5 and FeO_x/ZSM-5@SiO_2. The solid line is the desorption curve under 200 °C and the dashed line is the desorption curve under 350 °C.

for ZnO_x/ZSM-5 or for FeO_x/ZSM-5. Compared to the ZnO_x-based catalysts, FeO_x-based catalysts had higher density of Brönsted acids but much lower density of Lewis acids.

Catalytic performances of different catalysts were evaluated using the MTA reaction. Conversion of methanol with HZSM-5 was always close to 100% within 420 minutes (Fig. 2a). The doping of metal oxides or coating with the SiO_2 shell on ZSM-5 resulted in the decrease of both surface area and pore volume (ESI-5, Table S2†), which influenced the diffusion of the product molecules and therefore shortened the life time of the catalyst. In detail, doping of FeO_x did not change this trend, and the conversion of methanol was close to 100% within 300 min. Conversion of methanol with FeO_x/ZSM-5@SiO_2 decreased to 97% at 120 min but could remain above 90% within 240 min, due to the decreased strength of external acids by coating (Fig. 1b). In contrast, the conversion of methanol with ZnO_x/ZSM-5 did not remain constant at 60 min. Even worse, the deactivation of ZnO_x/ZSM-5@SiO_2 catalyst was accelerated, due to the decrease of surface area and pore volume after coating with the SiO_2 shell (ESI-5, Table S2†).

Previous results suggested that ZnO_x interacted with ZSM-5 to form stable acidic sites, compared to FeO_x or Ga_2O_3, and it may be preparation method dependent.[22] Similar trends were observed with the yield of aromatics with different catalysts (Fig. 2b). HZSM-5, FeO_x/ZSM-5, and FeO_x/ZSM-5@SiO_2 all exhibited longer life times for producing aromatics as compared to the ZnO_x-based catalyst. In detail, FeO_x-based catalyst exhibited higher yield of aromatics in the initial stage of the reaction as compared to HZMS-5. In addition, yields of aromatics with three catalysts (HZSM-5,

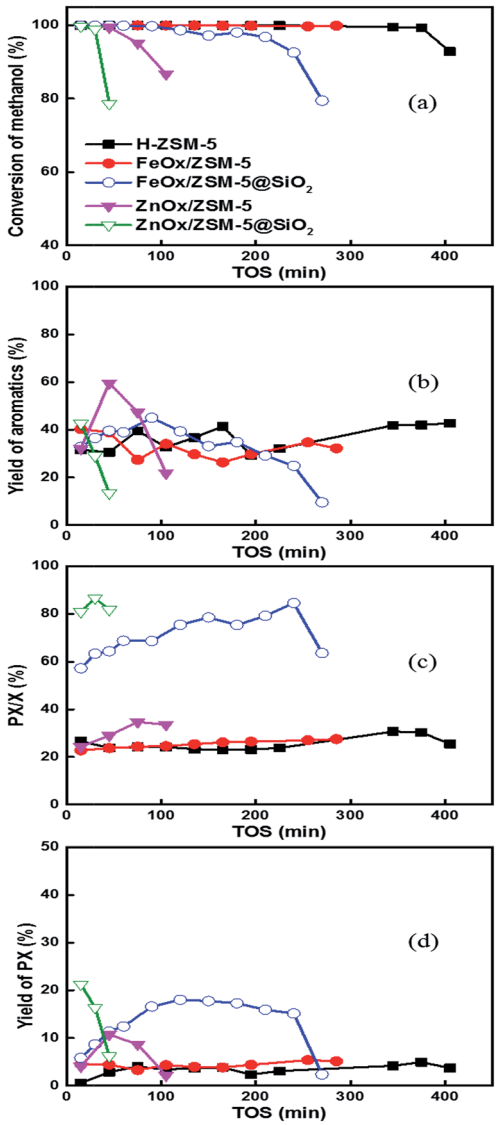

Fig. 2 (a) Conversion of methanol with different catalysts. (b) Yield of aromatics with different catalysts. (c) Selectivity of PX in X with different catalysts. (d) Yield of PX (carbon base) with different catalysts. The line and points with certain colours were all the same in (a) to (d).

FeO_x/ZSM-5, and FeO_x/ZSM-5@SiO_2) were very high in the initial stage. In sharp contrast, there is an obvious induction period for ZnO_x/ZSM-5. Yield of aromatics drastically increased from 15 to 60 minutes, reached the highest value at 60 minutes, but quickly dropped within 60–120 minutes. Yield of aromatics with ZnO_x/ZSM-5@SiO_2 drastically dropped from 15 to 30 minutes, showing a trend of rapid deactivation.

The coating effect with the SiO_2 shell on the selectivity of PX in X was studied, and the results are shown in Fig. 2c. For HZSM-5 and FeO_x/ZSM-5, this value is always 23–25% at very long times, close to the equilibrium ratio of PX in X with the catalyst with strong acids.[4,13,26–28] However, the value slightly increased with the reaction time using ZnO_x/ZSM-5, due to the coke deposition. In sharp contrast, coating of FeO_x/ZSM-5 with SiO_2 increased the selectivity of PX in X from 25% to 60% in the initial stage of the reaction, and the value sustainably increased to 80%, due to the gradual coke deposition with the reaction time.[4] Only when the pores of the catalyst were seriously blocked, the value decreased at 240–270 minutes. Using ZnO_x/ZSM-5@SiO_2, the selectivity of PX in X was directly increased to 80% from the pristine 25% and further increased to 90% at 60 minutes. Based on the selectivity of PX in X and the yield of X, we were able to calculate the yield of PX (carbon base, Fig. 2d). The yield of PX with FeO_x/ZSM-5@SiO_2 was around 3 times of those with HZSM-5 and FeO_x/ZSM-5. More strikingly, the gross yield of PX with FeO_x/ZSM-5@SiO_2, in single pass conversion, is 4–5 times that of ZnO_x/ZSM-5@SiO_2, owing to the longer life time of the former. The value also ranked as the highest value ever reported, validating that the SiO_2-coated FeO_x/ZSM-5 is a very promising catalyst for the production of PX in high yield. External acids of ZnO_x/ZSM-5 are approximately 3.27% of the total but decreased to 2.44% of the total after it was coated with the SiO_2 shell (ESI-5, Table S2†). In comparison, external acids of FeO_x/ZSM-5 are approximately 5.85% of the total but decreased to 1.81% after it was coated with the SiO_2 shell, qualitatively in agreement with the previous statement.[4,26–28] Density of external acids is 0.024 mmol g^{-1} and 0.013 mmol g^{-1} for ZnO_x/ZSM-5@SiO_2 and FeO_x/ZSM-5@SiO_2, respectively. The low value is key to the high selectivity of PX in X *via* the suppression of isomerization of X. In addition, coating the catalyst with the SiO_2 shell resulted in the significant decrease of both surface area and pore volume (ESI-5, Table S2†). Pores of the amorphous layer of SiO_2, studied with the adsorption of PX,[4] were in the range of 0.51–0.57 nm. ZSM-5 exhibited shape selectivity of *ortho*-xylene (OX), but not on PX, significantly dominating their decomposition behaviour on an external surface or in the internal pores of the zeolite.[4]

Furthermore, we compared the yield of olefins obtained using different catalysts (Fig. 3). The yield of ethylene with FeO_x/ZSM-5 is 3–5% higher than that obtained with HZSM-5. This value can be further increased by coating FeO_x/ZSM-5 with SiO_2. In comparison, the yield of ethylene with ZnO_x-based catalyst is much higher, but the trend could not remain stable for a long time (Fig. 3a). Interestingly, FeO_x-based catalyst gave higher yield of propylene, compared to HZSM-5 and ZnO_x-based catalysts (Fig. 3b). The difference in obtaining different yields of different olefins would be attributed to the dual hydrocarbon pool mechanism with different catalysts.[9–12] Actually, propylene is mostly produced from the olefin pool, nearly independently of the aromatics pool. Ethylene is mostly produced from the aromatics pool, which should exhibit similar change trends with the aromatic products.[12] The conclusion is supported by the change trends of aromatics and ethylene in Fig. 2b and 3a, respectively. For the yield of C_2–C_3 olefins and PX together (Fig. 3c), FeO_x/ZSM-5@SiO_2 exhibited highest gross yield, which is approximately 2 times that obtained using FeO_x/ZSM-5, 2.5 times that obtained using HZSM-5, and 3–4 times that obtained using ZnO_x/ZSM-5 and ZnO_x/ZSM-5@SiO_2.

In addition, the yields of C_2 or C_3 hydrocarbons with different catalysts were also compared (Fig. 4a and b). ZnO_x-based catalysts exhibited high yield of C_2 hydrocarbons but much lower yield of C_3 hydrocarbons, compared to HZSM-5 or

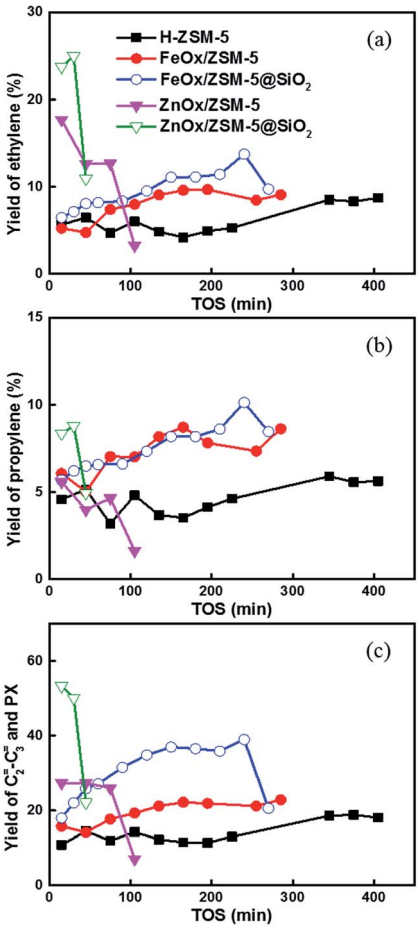

Fig. 3 (a) Time-dependent yield of ethylene with different catalysts. (b) Time-dependent yield of propylene with different catalysts. (c) Time-dependent gross yield of C_2–C_3 olefins and PX with different catalysts. The line and points with certain colours were all the same in (a) to (c).

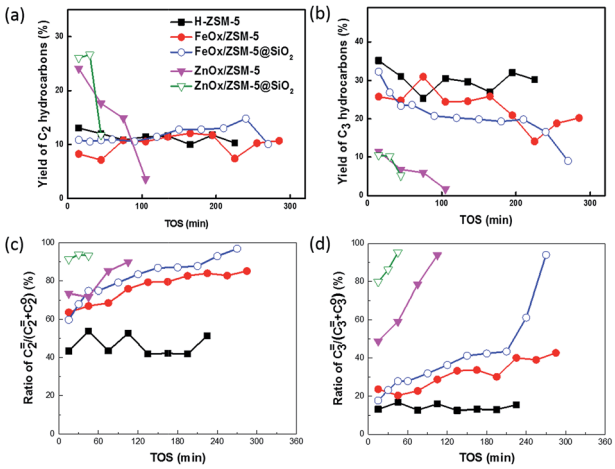

Fig. 4 (a) Yield of C_2 hydrocarbons with different catalysts at different times. (b) Yield of C_3 hydrocarbons with different catalysts at different times. (c) Ratio of ethylene to C_2 hydrocarbons with different catalysts at different times. (d) Ratio of propylene to C_3 hydrocarbons with different catalysts at different times. The line and points with certain colours were all the same in (a) to (d).

FeO_x-based catalysts. The yields of C_2 and C_3 hydrocarbons with FeO_x catalysts were similar to those obtained with HZSM-5. These results suggested that the aromatic pool and olefin pool can be tuned with catalysts with different acids. FeO_x/ZSM-5 had densities of Lewis acids and Brönsted acids similar to those of HZSM-5. They gave similar distribution of C_2 and C_3 hydrocarbons. In comparison, a high density of Lewis acids on ZnO_x-based catalysts enhanced the aromatic pool, considering that C_2 hydrocarbons were mostly produced from aromatics.[12] The yield of C_3 hydrocarbons with ZnO_x/ZSM-5 is only 1/3 of that obtained with HZM-5, suggesting that the olefin pool was significantly suppressed with ZnO_x-based catalysts. In addition, the ratios of ethylene to C_2 hydrocarbons (ethylene and ethane) and propylene to C_3 hydrocarbons (propylene and propane) were calculated (Fig. 4c and d). The modification of ZSM-5 with ZnO_x and FeO_x increased the ratio of ethylene/(ethylene and ethane), compared to HZSM-5. It validated the suppression of hydrogen transfer of olefins, and the enhancement of the aromatization could be simultaneously realized. Quantitatively, coating of FeO_x/ZSM-5 with SiO_2 resulted in the ratio of ethylene to C_2 hydrocarbons increasing by 10–15%. Moreover, selectivity of PX in X is increased by 55–60%. Reasonably, the isomerization of X mainly occurred at the external surface of the catalyst and not inside the pores, due to the shape selectivity of ZSM-5.[5] However, the hydrogen transfer reaction of ethylene mainly occurred inside the pores, considering that the inner surface area of microsized ZSM-5 is far larger than that of the external surface. However, the hydrogen transfer of propylene would be effectively suppressed using the catalysts with the SiO_2 shell. Since propylene had a diffusion rate slower than that of ethylene, the contact between them with the external surface of the catalyst would exhibit a significant effect on their selectivity, compared to that of the smaller molecule.[29]

In addition, the relation between the acidity information and the catalytic performance of the catalysts also suggested that Lewis acids in large amounts with ZnO_x/ZSM-5 resulted in the increased yield of aromatics and ethylene, but shortened the lifetime of the catalyst. FeO_x/ZSM-5 with slightly higher amount of Brönsted acids and less amount of Lewis acids exhibited higher yield of aromatics and longer lifetime. The difference may be attributed to the interaction of ions of Zn^{2+} and ions of Fe^{+}, Fe^{2+}, and Fe^{3+} with the ZSM-5. Further investigation is needed to develop an understanding of the different acids with different catalysts. Moreover, the syngeneic effect, by coating FeO_x/ZSM-5 with the SiO_2 shell, gave a better catalyst than ZnO_x-based catalyst, in terms of producing a higher gross yield of C_2–C_3 olefins and PX for long times (Fig. 3c).

In summary, we evaluated that the FeO_x-doped ZMS-5 exhibited better performance in terms of stability in high temperature reaction. Coating the catalyst with the SiO_2 shell effectively suppresses the isomerization of X and the hydrogen transfer of propylene on an external surface of the catalyst.

FeO_x/ZSM-5@SiO_2 exhibited longer life time to produce C_2–C_3 olefins and PX in far higher gross yield, compared to other catalysts. It was also validated that the catalyst with high density of Lewis acids was easily deactivated as compared to the catalyst

with both Brönsted acids and Lewis acids with medium strength. These results were useful for the further control of the product selectivity in methanol-to-aromatics process.

Acknowledgements

The authors thank the support of NSFC program (21376135, 91434122 and 51236004).

Notes and references

1 M. Stöcker, *Microporous Mesoporous Mater.*, 1999, **29**, 3–48.
2 S. T. Xu, A. M. Zheng, Y. X. Wei, J. R. Chen, J. Z. Li, Y. Y. Chu, M. Z. Zhang, Q. Y. Wang, Y. Zhou, J. B. Wang, F. Deng and Z. M. Liu, *Angew. Chem., Int. Ed.*, 2013, **125**, 11778–11782.
3 Y. X. Li, M. Y. Zhang, D. Z. Wang, F. Wei and Y. Wang, *J. Catal.*, 2014, **311**, 281–287.
4 J. G. Zhang, W. Z. Qian, C. Y. Kong and F. Wei, *ACS Catal.*, 2015, **5**, 2982–2988.
5 Y. Bhawe, M. Moliner-Marin, J. D. Lunn, Y. Liu, A. Malek and M. Davis, *ACS Catal.*, 2012, **2**, 2490–2495.
6 J. Zhou, J. W. Teng, L. P. Ren, Y. D. Wang, Z. C. Liu, W. Liu, W. M. Yang and Z. K. Xie, *J. Catal.*, 2016, **340**, 166–176.
7 J. F. Haw, J. B. Nicholas, W. G. Song, F. Deng, Z. K. Wang, T. Xu and C. S. Heneghan, *J. Am. Chem. Soc.*, 2000, **122**, 4763–4775.
8 D. L. Cai, Q. Wang, Z. Jia, Y. H. Ma, Y. Cui, U. Muhammad, Y. Wang, W. Z. Qian and F. Wei, *Catal. Sci. Technol.*, 2016, **6**, 1297–1301.
9 S. Ilias and A. Bhan, *J. Catal.*, 2012, **290**, 186–192.
10 U. Olsbye, S. Svelle, M. Bjorgen, P. Beato, T. V. Janssens, F. Joensen, S. Bordiga and K. P. Lillerud, *Angew. Chem., Int. Ed.*, 2012, **51**, 5810–5831.
11 S. Svelle, F. Joensen, J. Nerlov, U. Olsbye, K. P. Lillerud, S. Kolboe and M. Bjørgen, *J. Am. Chem. Soc.*, 2006, **128**, 14770–14771.
12 R. Khare and A. Bhan, *J. Catal.*, 2015, **329**, 218–228.
13 T. Wang, X. P. Tang, X. F. Huang, W. Z. Qian, Y. Cui, X. Y. Hui, W. Yang and F. Wei, *Catal. Today*, 2014, **233**, 8–13.
14 D. Freeman, R. P. K. Well and G. J. Hutchings, *J. Catal.*, 2002, **205**, 358–365.
15 N. Wang, W. Z. Qian, K. Shen, C. Su and F. Wei, *Chem. Commun.*, 2016, **52**, 2011–2014.
16 J. A. Lopez-Sanchez, M. Conte, P. Landon, W. Zhou, J. K. Bartley, S. H. Taylor, A. F. Carley, C. J. Kiely, K. Khalid and G. J. Hutchings, *Catal. Lett.*, 2012, **142**, 1049–1056.
17 Y. Inoue, K. Nakashiro and Y. Ono, *Microporous Mater.*, 1995, **4**, 379–383.
18 Y. H. Ma, N. Wang, W. Z. Qian, Y. Wang, J. M. Zhang and F. Wei, *RSC Adv.*, 2016, **6**, 81198–81202.
19 K. Shen, W. Z. Qian, N. Wang, C. Su and F. Wei, *J. Am. Chem. Soc.*, 2013, **135**, 15322–15325.
20 K. Shen, W. Z. Qian, N. Wang, J. Zhang and F. Wei, *J. Mater. Chem. A*, 2013, **1**, 3272–3275.
21 K. Shen, W. Z. Qian, N. Wang, C. Su and F. Wei, *J. Mater. Chem. A*, 2014, **2**, 19797–19808.
22 El-M. El-Malki, R. A. van Santen and W. M. H. Sachtler, *J. Phys. Chem. B*, 1999, **103**, 4611–4622.
23 S. M. T. Almutairi, B. Mezari, P. C. M. M. Magusin, E. A. Pidko and E. J. M. Hensen, *ACS Catal.*, 2012, **2**, 71–83.
24 R. Roesky, J. Weiguny, H. Bestgen and U. Dingerdissen, *Appl. Catal., A*, 1999, **176**, 213–220.
25 S. Pin, M. A. Newton, F. D. Acapito, M. Zema, S. C. Tarantino, G. Spinolo, R. A. De Souza, M. Martin and P. Ghigna, *J. Phys. Chem. C*, 2012, **116**, 980–986.
26 J. H. Ahn, R. Kolvenbach, S. S. Al-Khattaf, A. Jentysa and J. A. Lercher, *Chem. Commun.*, 2013, **49**, 10584–10586.
27 A. Ghorbanpour, A. Gumidyala, L. C. Grabow, S. P. Crossley and J. D. Rimer, *ACS Nano*, 2015, **9**, 4006–4016.
28 T. Otto, S. I. Zones and E. Iglesia, *J. Catal.*, 2016, **339**, 195–208.
29 F. L. Bleken, S. Chavan, U. Olsbye, M. Boltz, F. Ocampo and B. Louis, *Appl. Catal., A*, 2012, **447**, 178–185.

